

Spontaneous Formation of Nanostructures in $\text{In}_x\text{Ga}_{1-x}\text{As}$ Epilayers Grown by Molecular Beam Epitaxy on GaAs Non-(100)-Oriented Substrates

Pablo O. VACCARO, Kazuhisa FUJITA and Toshihide WATANABE

*ATR Optical and Radio Communications Research Laboratories
2-2 Hikaridai, Seika-cho, Soraku-gun, Kyoto 619-02, Japan
e-mail: vaccaro@acr.atr.co.jp*

$\text{In}_x\text{Ga}_{1-x}\text{As}$ was deposited by MBE on GaAs (100), (111)A-, (211)A- and (311)A-oriented substrates. The strained epilayers formed a variety of three-dimensional surfaces. An $\text{In}_{0.5}\text{Ga}_{0.5}\text{As}$ epilayer grown on a (311)A-oriented substrate shows a corrugated nanostructure with a period of 35 nm. An $\text{In}_{0.75}\text{Ga}_{0.25}\text{As}$ epilayer grown on a (111)A-1° off-oriented substrate shows a surface covered by platelets. Another epilayer grown on a (211)A-oriented substrate shows faceted islands. These results show that the growth of strained layers on non-(100)-oriented substrates is a promising path to obtain spontaneously formed nanostructures.

1. INTRODUCTION

The growth of highly strained semiconductor epilayers has shown to be a rich field for finding nanostructures spontaneously formed^{1,2}). Most of these growths were performed on the usual (100)-oriented substrates. Since the substrate orientation is a key factor in the formation of the nanostructures^{3,4}), we decided to investigate the growth of highly strained InAs epilayers on non-(100)-oriented substrates. The accumulated strain energy due to the large mismatch between GaAs and $\text{In}_x\text{Ga}_{1-x}\text{As}$ for high x values determines that only a few monolayers of $\text{In}_x\text{Ga}_{1-x}\text{As}$ can be grown before reaching the critical thickness where the epilayer relaxes by formation of dislocations. The dislocations are efficient non-radiative recombination centers that deteriorate the optical and electrical properties of the nanostructures. Therefore, we constrained our investigation to epilayers not thicker than a few monolayers.

2. EXPERIMENTAL

The samples were grown by molecular beam epitaxy on GaAs substrates with the following orientations: (100), (311)A, (211)A, and (111)A just, 1° off toward [100]. All the substrates had a 300 nm thick GaAs buffer layer grown at 550°C with an As₄ beam equivalent pressure (BEP) of 2.5×10^{-5} Torr. $\text{In}_x\text{Ga}_{1-x}\text{As}$ was grown at 500°C with an As₄ BEP of 0.9×10^{-5} Torr.

The structure grown on the (311)A and (100)-oriented substrates consisted nominally of an $\text{In}_{0.15}\text{Ga}_{0.85}\text{As}$ strained quantum well of 3 nm thickness for reference in the optical measurements and the nanostructured $\text{In}_{0.5}\text{Ga}_{0.5}\text{As}$ layer separated by GaAs spacers. The $\text{In}_{0.5}\text{Ga}_{0.5}\text{As}$ layer was grown in 24 cycles of one second of $\text{In}_{0.5}\text{Ga}_{0.5}\text{As}$ and three seconds As₄ pause to promote the formation of nanostructures⁴). The total amount of $\text{In}_{0.5}\text{Ga}_{0.5}\text{As}$ is about 6 monolayers or 1.7 nm. Sets of samples with 2, 4, 6, and 8 monolayers of InGaAs and without cap layer were grown using the same growth procedure to perform atomic force microscopy (AFM) measurements. Photoluminescence was measured by using a tunable Ti-sapphire laser (300 fsec pulses at 82 MHz repetition rate, 750 nm wavelength, 250 mW average power) for excitation, and a monochromator and a streak camera (5 psec resolution) for detection.

The structures grown on the other substrates consisted nominally of 4 monolayers of $\text{In}_{0.75}\text{Ga}_{0.25}\text{As}$ or 12.5 monolayers of $\text{In}_{0.25}\text{Ga}_{0.75}\text{As}$. These thicknesses were chosen to have similar strain energies in all the samples.

3. RESULTS AND DISCUSSION

The (100)-oriented samples with 2 and 4 monolayers of InGaAs show a flat surface when observed by AFM. The (100)-oriented samples with 6 and 8 monolayers of InGaAs show islands with a diameter of 25 nm and a height of 3 nm, in agreement with previous works¹). The island density as counted directly from the AFM pictures is 5.5×10^9 islands/cm² for the sample with 6 monolayers of InGaAs. This set of samples shows the usual Stranski-Krastanow growth mode. The growth of the strained epilayer begins layer-by-layer and changes to a three-dimensional growth above a critical thickness of about 6 monolayers, for this In content. On the other hand, the (311)A-oriented samples with 2, 4, and 6 monolayers of InGaAs show an increasingly corrugated surface, as shown in Fig. 1 (a), (b), and (c). The sample with 2 monolayers of InGaAs (Fig. 1 (a)) shows a short-period corrugation of about 3 nm period and 0.3-0.5 nm height. As the InGaAs layer becomes thicker, a large-period corrugation (about 35 nm period and 2 nm height) develops (Fig. 1 (b)), until reaching its best shape for a 6 monolayers thickness (Fig. 1 (c)). Further growth produces the Stranski-Krastanow transformation. The sample with 8 monolayers (Fig. 1 (d)) shows a surface covered with three-dimensional islands that are similar to the ones observed on the (100)-oriented samples for 6 monolayers.

Figure 2 shows the radiative recombination time constant dependence on temperature for nanostructures and conventional quantum wells grown on (311)A and (100) substrates. The radiative recombination time was obtained from the measured photoluminescence decay time and photoluminescence intensity using the model of Gurioli *et al.*⁵). Data for conventional quantum wells (filled symbols) are taken from Takahashi *et al.*⁶), where the difference between (311)A and (100) radiative recombination times is explained. These conventional quantum wells show the usual increase of radiative recombination time with temperature⁵).

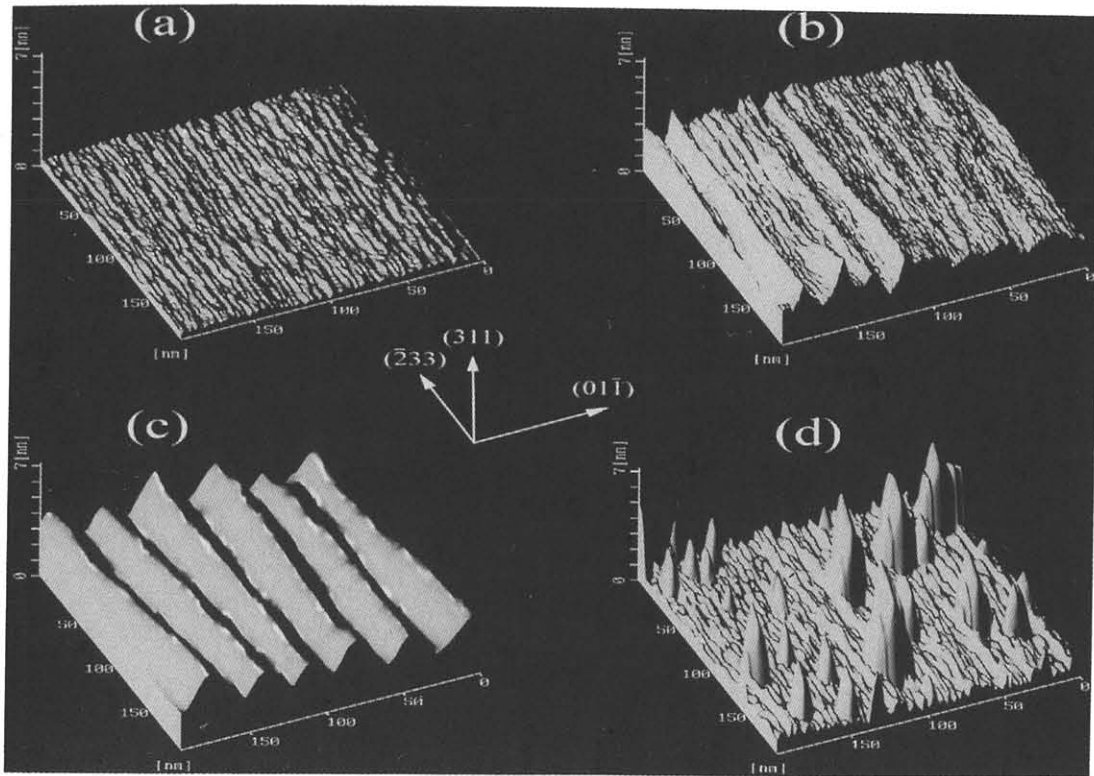


Fig. 1. AFM images of $\text{In}_{0.5}\text{Ga}_{0.5}\text{As}$ layers grown on GaAs (311)A-oriented substrates. The thickness of the layer is: (a) 2 monolayers; (b) 4 monolayers; (c) 6 monolayers; and (d) 8 monolayers.

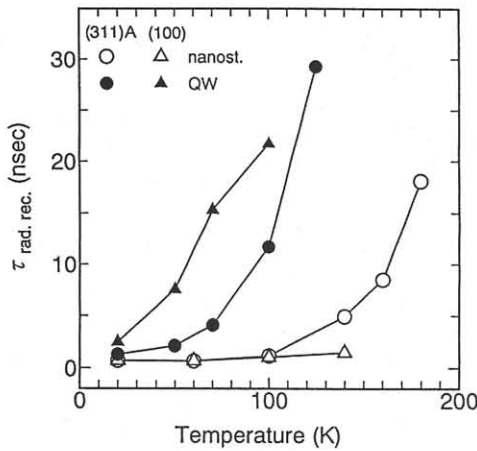


Fig. 2. Radiative recombination time constant dependence on time for nanostructures and conventional quantum wells grown on (311)A and (100) substrates.

Excitons are thermally excited to higher states where radiative recombination is not allowed because momentum conservation, therefore only a small fraction of excitons which have lower momentum can recombine radiatively as temperature increases.

On the other hand, the (100) sample which has quantum dots shows very little increase of radiative recombination time with temperature. This behavior shows that there are not states where excitons can be thermally excited in this temperature range, i.e., there is a gap in the density of states of the quantum dots between the fundamental level and the excited levels as predicted by theory. Besides, the short radiative recombination time (less than 1 nsec up to 140 K) is very promissory for application in light emitting devices.

The (311)A sample which has the corrugated nanostructure also shows little increase of the radiative recombination time up to 100 K, indicating the presence of a gap in the density of states. The steep increase for higher temperatures shows that excitons are excited to states with higher momentum from where radiative recombination is not allowed. We estimate from the exponential increase of the radiative recombination time that the energy gap between the fundamental and the first excited level is less than 10 meV. The experimental temperature dependence of radiative recombination time for the corrugated sample is similar to the one expected for quantum dots, and it does not agree with the dependence theoretically predicted for quantum wires⁵). The radiative recombination time for quantum wires should show a fast increase at low temperatures and a slower increase at higher temperatures. Therefore we suppose that excitons are localized in the thicker regions of the wire-like structure at low temperature and they become excited to non-localized states as temperature increases above 100 K. This view is supported also by the small value of the activation energy for increase of the radiative time constant (less than 10 meV).

Figure 3 shows the surface of an $\text{In}_{0.75}\text{Ga}_{0.25}\text{As}$ epilayer with four monolayers of thickness grown on a (111)A-1° off-oriented substrate. The surface is covered by small InGaAs platelets whose surface is tilted between one or two degrees respect to the surface. The average spacing of the platelets' rows is 36 nm and the height at the front edge is about 0.7 nm. The ideal separation between monolayer steps on the GaAs (111)A-1° off-oriented substrate is 19 nm for a monolayer thickness of 0.331 nm. Therefore, the platelets observed in this sample are formed by two monolayers bunched together. The morphology of this sample suggests that the InGaAs

grows in the step-flow growth mode. It is remarkable that the steep edge of the platelets has always a two monolayers height and that one monolayer height is not observed.

Figure 4 shows the surface of an $\text{In}_{0.75}\text{Ga}_{0.25}\text{As}$ epilayer with four monolayers of thickness grown on a (211)A-oriented substrate. The surface is covered with faceted islands with a size between 2 nm and 20 nm, elongated in the [222] direction. The angle between the long-sides facets and the substrate is about 40-50°, and the angle between the short-sides facets and the substrate is about 15-30°.

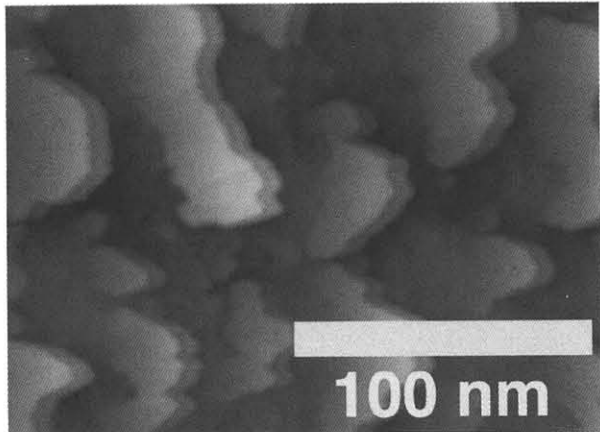


Fig. 3. AFM image of four monolayers of $\text{In}_{0.75}\text{Ga}_{0.25}\text{As}$ grown on GaAs (111)A-1° off-oriented substrate.

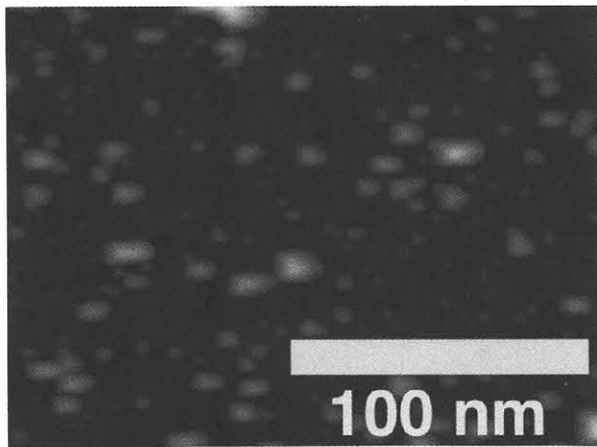


Fig. 4. AFM image of four monolayers of $\text{In}_{0.75}\text{Ga}_{0.25}\text{As}$ grown on GaAs (211)A-oriented substrate.

Figure 5 shows the surface of an $\text{In}_{0.25}\text{Ga}_{0.75}\text{As}$ epilayer with 12.5 monolayers of thickness grown on a (211)A-oriented substrate. The dot-like surface features have about 1 nm of height and an areal density of $3.3 \times 10^{12} \text{ cm}^{-2}$. The height of the dots is much smaller than the total InGaAs thickness (about 4 nm), therefore, there is a continuous InGaAs layer below this nanostructure.

These four cases of nanostructures formed on non-(100)-oriented substrates appear as a consequence of various mechanisms. The Stranski-Krastanow growth mode for strain relaxation, observed in Fig. 2 and 4, is one of them. Step-flow growth mode and spontaneous formation of facets are also important in Fig. 2 and 3. The formation mechanism of the nanostructure of Fig. 5

is not clear. The mechanisms mentioned before are susceptible to be controlled by modifying the growth conditions and nanostructures with high crystal quality and required shapes can be obtained.

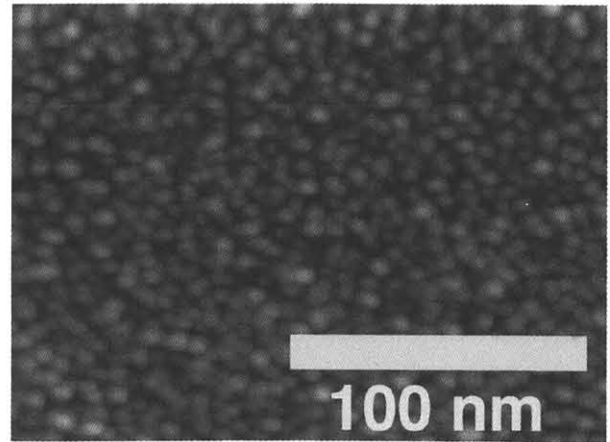


Fig. 5. AFM image of 12.5 monolayers of $\text{In}_{0.25}\text{Ga}_{0.75}\text{As}$ grown on GaAs (211)A-oriented substrate.

4. CONCLUSIONS

A corrugated quantum well structure with 35 nm period was obtained by growing $\text{In}_{0.5}\text{Ga}_{0.5}\text{As}$ on GaAs (311)A-oriented substrates in the same conditions used to grow self-assembled quantum dots on GaAs (100) oriented substrates. The temperature dependence of the radiative recombination time constant of the (100) sample agrees with that predicted for quantum dots. On the other hand, the temperature dependence of the radiative recombination time of the (311)A sample shows that its density of states does not correspond to the density of states predicted for quantum wires. It seems to be similar to the density of states of a 0-D confinement structure (quantum dots). We attribute this result to the lack of uniformity along the wire-like structure that produces a potential modulation enough to confine carriers in 0-D.

InGaAs epilayers grown on (211)A and (111)A-1° off-oriented substrates also showed the formation of interesting nanostructures. These nanostructures appear because a combination of mechanisms, as Stranski-Krastanow growth mode, step-flow growth mode, and faceting. These results show that growth of strained layers on non-(100)-oriented substrates is a promising path to obtain spontaneously formed nanostructures.

References

- 1) D. Leonard M. Krishnamurthy, S. Fafard, J. L. Merz and P. M. Petroff: J. Vac. Sci. Technol. **B12** (1994) 1063.
- 2) J. -Y. Marzin, J. -M. Gerard, A. Izrael, D. Barrier and G. Bastard: Phys. Rev. Lett. **73** (1994) 716.
- 3) R. Notzel, J. Temmyo and T. Tamamura: Appl. Phys. Lett., **64** (1994) 3557.
- 4) E. Tournié and R. Nötzel: Appl. Phys. Lett. **63** (1993) 3300.
- 5) M. Gurioli, A. Vinattieri, M. Colocci, C. Deparis, J. Massies, G. Neu, A. Bosacchi and S. Franchi: Phys. Rev. **B44** (1991) 3115.
- 6) M. Takahashi, P. O. Vaccaro, K. Fujita and T. Watanabe: Appl. Phys. Lett. **66** (1994) 93.